

## Performance Analysis of a Speed Sensorless Induction Motor Drive Based on DTC Scheme

S. Belkacem, F. Naciri, R. Abdessemed and B. Kiyyour  
 LEB-Research Laboratory, Department of Electrical Engineering, University of Batna,  
 Street Chahid M<sup>ed</sup> El Hadi Boukhrouf, 05000, Algeria

**Abstract:** This study presents a method for estimation of the stator flux components and rotor speed based on the theory of an adaptive control and a Direct Torque Control (DTC). A linear observer for estimation of the stator flux is synthesized, by using a Lyapunov theory in order to guarantee stability for state estimation. The adaptive observer is associated to a direct torque control of an induction motor. To illustrate the performances and the robustness of this observer, a simulation results is presented.

**Key words:** DTC, adaptive speed and flux observer, regulator design, sensorless control

### INTRODUCTION

Estimation can be defined as: the determination of constants or variables for any system, according to a performance level and based in the measurements taken from the process (Lasca *et al.*, 2000).

Since its introduction in 1985, the Direct Torque Control (DTC) (Takahashi and Noguchi, 1986) principle was widely used for IM drives with fast dynamics. Despite its simplicity, DTC is able to produce very fast torque and flux control, if the torque and the flux are correctly estimated, is robust with respect to motor parameters and perturbations.

As it is well known, speed sensors like tachometers or incremental encoders increase the size and the cost of systems unnecessarily. Similar problems arise with the addition of search coils or Hall Effect sensors to the motor for the measurement of flux, hindering functionality in terms of implementation. Thus, to improve the overall system performance, state estimators or observers are usually more preferable than physical measurements (Morand, 2005; Casadei *et al.*, 2002; Elbuluk and Kankam, 1997).

Recently, the emphasis of research on induction motor drives has been on sensorless drive, which eliminates flux and speed sensors mounted on the motor. Also, the development of effective speed and flux estimators has allowed good Rotor Flux-Oriented (RFO) performance at all speeds except those close to zero. Sensorless control has improved the motor performance, compared to the Volts/Hertz (or constant flux) controls (Bottiglieri *et al.*, 2003).

The objectives of sensorless drives control are:

- Reduction of hardware complexity and cost,
- Increased mechanical robustness,
- Operation in hostile environments,
- Higher reliability,
- Increased noise immunity,
- Unaffected machine inertia.

Adaptive speed observers seem to be between the most promising methods thanks to their good performance versus computing time ratio. They have the advantage to provide both flux and mechanical speed estimates without problems of open-loop integration. Besides, the adaptive observer has the interesting property to provide a mechanism for on-line tuning of key model parameters such as the stator or rotor resistance.

For the speed regulation, the saturation of the manipulated variable can involve a phenomenon of racing of the integral action during the great variations (starting of the machine), which is likely to deteriorate the performances of the system or even to destabilize it completely, the solution consists in correcting the integral action.

### MODELLING OF THE INDUCTION MOTOR

In this study, the induction motor model is given by, (Canudas, 2000)

$$\begin{cases} \dot{x} = Ax + BU \\ y = Cx \end{cases} \quad (1)$$

Where

$$x = [i_{s\alpha} \ i_{s\beta} \ \Psi_{r\alpha} \ \Psi_{r\beta}]^T$$

$$y = [i_{s\alpha} \ i_{s\beta}]^T, \quad U = [V_{s\alpha} \ V_{s\beta}]^T$$

$$C = \begin{bmatrix} 1 & 0 & 0 & 0 \\ 0 & 1 & 0 & 0 \end{bmatrix}^T, \quad K = \begin{bmatrix} M \\ sL_s L_r \end{bmatrix}$$

$$\gamma = \begin{bmatrix} R_s + R_r M^2 \\ \sigma L_s \quad L_r^2 \sigma L_s \end{bmatrix}$$

$$A = \begin{bmatrix} -\gamma & 0 & \frac{K}{T_r} & K\omega_r \\ 0 & -\gamma & -K\omega_r & \frac{K}{T_r} \\ \frac{M}{T_r} & 0 & -\frac{K}{T_r} & -\omega_r \\ 0 & \frac{M}{T_r} & \omega_r & -\frac{K}{T_r} \end{bmatrix}, \quad B = \begin{bmatrix} \frac{1}{\sigma L_s} & 0 \\ 0 & \frac{1}{\sigma L_s} \\ 0 & 0 \\ 0 & 0 \end{bmatrix}$$

### PRINCIPLE OF THE DTC

DTC is a control philosophy exploiting the torque and flux producing capabilities of ac machines when fed by a voltage source inverter that does not require current regulator loops, still attaining similar performance to that obtained from a vector control drive.

**Behavior of stator flux:** In the reference  $(\bullet, \bullet)$ , the stator flux can be obtained by the following equation:

$$\bar{V}_s = R_s \bar{I}_s + \frac{d}{dt} \bar{\Psi}_s \quad (2)$$

By neglecting the voltage drop due to the resistance of the stator to simplify the study (for high speeds), we find:

$$\bar{\Psi}_s \approx \bar{\Psi}_{s0} + \int_0^t \bar{V}_s dt \quad (2)$$

For one period of sampling, the voltage vector applied to the asynchronous machine remains constant, we can write:

$$\bar{\Psi}_s(k+1) \approx \bar{\Psi}_s(k) + \bar{V}_s T_e \quad (4)$$

Table 1: Selection for basic direct torque control

$\bullet \bullet$	$s$	$\bullet C_e$	$S_1$	$S_2$	$S_3$	$S_4$	$S_5$	$S_6$
1	1	1	$V_2$	$V_3$	$V_4$	$V_5$	$V_6$	$V_1$
0	0	0	$V_7$	$V_0$	$V_7$	$V_0$	$V_7$	$V_0$
		-1	$V_6$	$V_1$	$V_2$	$V_3$	$V_4$	$V_5$
0	1	0	$V_3$	$V_4$	$V_5$	$V_6$	$V_1$	$V_2$
		0	$V_0$	$V_7$	$V_0$	$V_7$	$V_0$	$V_7$
		-1	$V_3$	$V_6$	$V_1$	$V_2$	$V_3$	$V_4$

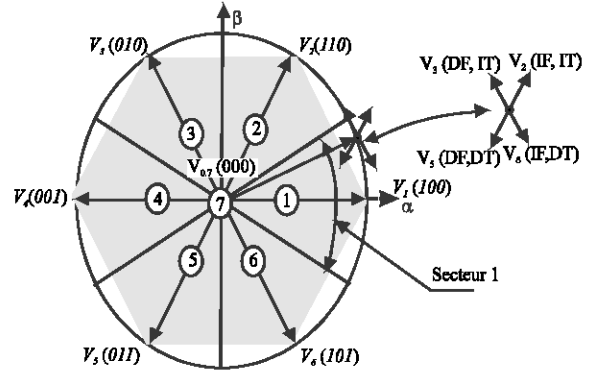


Fig. 1: Partition of the complex plan in 6 angular sectors  $S_{I=1 \dots 6}$

**Behavior of the torque:** The electromagnetic torque is proportional to the vector product between the stator and rotor flux according to the following expression:

$$C_e = k(\bar{\Psi}_s \times \bar{\Psi}_r) = k |\Psi_s| |\Psi_r| \sin(\delta) \quad (5)$$

**Development of the commutation strategy:** Table 1 shows the commutation strategy suggested by Takahashi and Noquchi (1986) to control the stator flux and the electromagnetic torque of the induction motor.

The Fig. 1 gives the partition of the complex plan in 6 angular sectors  $S_{I=1 \dots 6}$ .

IT: Increase the Torque, DT: Decrease the Torque.

IF: Increase the Flux, DF: Decrease the Flux.

### ADAPTIVE FLUX AND SPEED OBSERVER

A linear state observer for the stator flux can then be derived as follows, by considering the mechanical speed as constant parameter:

$$\hat{\dot{X}}_s = A\hat{X}_s + BU + G(\hat{i}_s - i_s) \quad (6)$$

The symbol  $\hat{\phantom{x}}$  denotes estimated values and  $G$  is the observer gain matrix.

We can estimate the rotor speed by using an adaptation mechanism. The system states and the parameters can also be estimate. The speed adaptation

mechanism is deduced by using a Lyapunov theory. The estimation error of the stator current and the rotor flux represents the difference between the observer and the model of the motor. The dynamic error is given by, Elbuluk and Kankam (1997), Maes and Melkebeek (2000).

$$\frac{d}{dt}e = (A + GC)e + \Delta A\hat{x} \quad (7)$$

where:

$$e = x - \hat{x} \quad (8)$$

$$\Delta A = A - \hat{A} = \begin{bmatrix} 0 & 0 & 0 & pK\Delta\omega_r \\ 0 & 0 & -pK\Delta\omega_r & 0 \\ 0 & 0 & 0 & -p\Delta\omega_r \\ 0 & 0 & p\Delta\omega_r & 0 \end{bmatrix} \quad (9)$$

$$\Delta w_r = w_r - \hat{w}_r \quad (10)$$

We consider the following Lyapunov function,

$$V = e^T e + \frac{1}{\lambda}(\Delta w_r)^2 \quad (11)$$

Whereis  $\lambda$  a positive constant, the derivative of Lyapunov function is giving as fellow:

$$\begin{aligned} \frac{d}{dt}V = e^T \{ & (A(w_r) + GC)^T + (A(w_r) + GC) \} e \\ & - 2K\Delta w_r (e_1 \hat{x}_4 - e_2 \hat{x}_3) + \frac{2}{\lambda} \Delta w_r \dot{\hat{w}}_r \end{aligned}$$

With  $\hat{\omega}_r$  is the estimated rotor speed. From Eq. 11, we can deduce the adaptation law for the estimation of the rotor speed by the equality between the second and the third term, we obtain:

$$\dot{\hat{\omega}}_r = \lambda K(e_1 \hat{x}_4 - e_2 \hat{x}_3) \quad (13)$$

With K is a positive constant To enhance the dynamic behavior of the speed observer, we added a proportional term. The speed adaptation laws become:

$$\dot{\hat{\omega}}_r = k_p (e_1 \hat{x}_4 - e_2 \hat{x}_3) + k_i \int_0^t (e_1 \hat{x}_4 - e_2 \hat{x}_3) dt \quad (14)$$

Where  $k_p$  and  $k_i$  are positive gains.

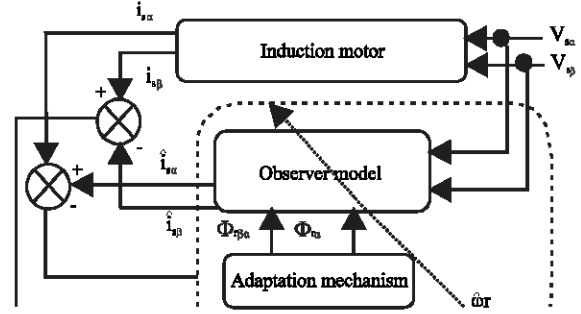


Fig. 2: Global adaptive observer structure

**Synthesis of the adaptive observer:** To solve the problem related especially to the estimation of the components of stator flux and the rotor speed we have recourse to adaptive observer; the adaptation mechanism is a PI regulator.

The block diagram of the observer with the adaptive mechanism is given in Fig. 2.

**Observer gain selection:** The observer gain matrix is chosen so that to impose a fast dynamic for the observer. The observer matrix is presented as follow (Casadei *et al.*, 2003; Akin, 2003)

$$G = \begin{bmatrix} g_1 & -g_2 \\ g_2 & g_1 \\ g_3 & -g_4 \\ g_4 & g_3 \end{bmatrix} \quad (15)$$

Where  $g_1, g_2, g_3, g_4$ , are given by:

$$g_1 = (1 - k_1) \left( \frac{R_s}{\sigma L_s} + \frac{1 - \sigma}{\sigma T_r} + \frac{1}{T_r} \right),$$

$$g_2 = (k_1 - 1) \hat{\omega}_r$$

With  $k_1$  is a coefficient obtained by pole placement.

### SYSTEM OF SPEED REGULATION

The saturation of the manipulated variable can involve a phenomenon of racing of the integral action during the great variations (starting of the machine), which is likely to deteriorate the performances of the system or even to destabilize it completely. To overcome this phenomenon, a solution consists in correcting the integral action according to the diagram of Fig. 3. The correction of the integral action is based on the difference between the values of  $(\bullet)$  upstream and downstream from the limiting device, balanced by the coefficient  $1/k \bullet$  such as Cao *et al.* (2002), Zaccarian and Teel (2004).

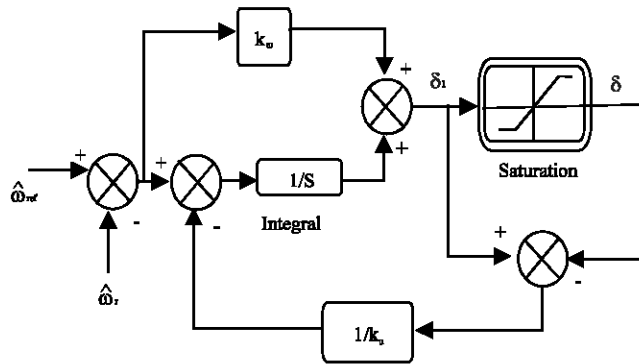


Fig. 3: Structure of the anti-windup PI system

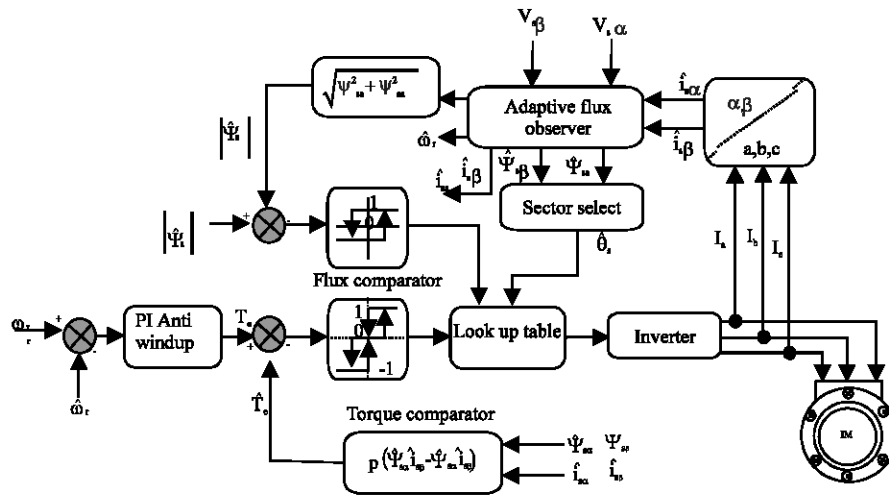


Fig. 4: Speed sensorless DTC system using adaptive flux observer

The stator flux is a function of the rotor flux which is represented by:

$$\begin{cases} \Psi_{s\alpha} = sL_s i_{s\alpha} + \frac{M}{L_r} \Psi_{r\alpha} \\ \Psi_{s\beta} = sL_s i_{s\beta} + \frac{M}{L_r} \Psi_{r\beta} \end{cases} \quad (16)$$

### PROPOSED SENSORLESS INDUCTION MOTOR DRIVE

The proposed sensorless IM drive block diagram is shown in Fig. 4. The drive operates at constant stator flux uses DTC to provide torque control. The speed controller is a anti-windup PI regulator that generates the reference torque. Measurements of two line currents and the average voltage over a PWM switching period are used

P = 4 KW	f = 50 Hz	W <sub>r</sub> = 1440 rpm	V <sub>i</sub> = 380 V
R <sub>s</sub> = 1.2•	R <sub>r</sub> = 1.8•	L <sub>s</sub> = 0.1554 H	L <sub>r</sub> = 0.1568 H
T <sub>r</sub> = 0.0871s	M = 0.15 H	J = 0.07 kgm <sup>2</sup>	P = 2

in the adaptive flux observer and the direct torque control. The stator flux is estimated by the adaptive observer and used in the DTC control. The IM under study is a 4-kw two-pole squirrel-cage motor; the parameters are listed in Table 2.

### SENSITIVITY STUDY AND SIMULATION RESULTS

The sensorless IM drive of Fig. 4 was verified using simulations. During the simulations, the torque set value is limited to 25N.m (rated torque), In order to show the performances and the robustness of the adaptive observer, we simulated different cases, which are

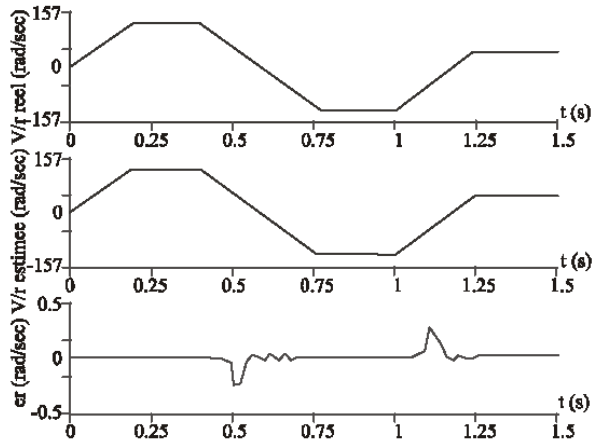


Fig. 5: Actual, estimated speed and estimation error

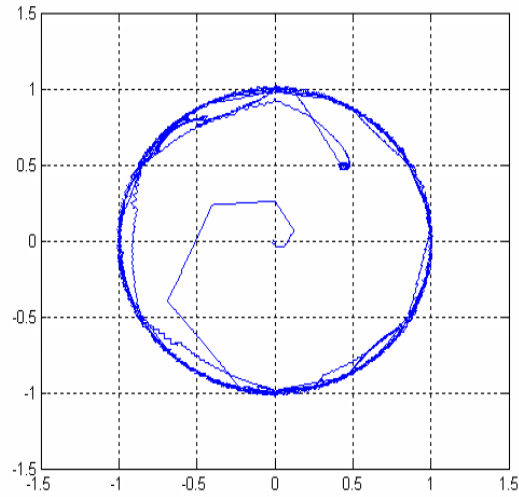


Fig. 8: Trajectory of the estimated stator flux components

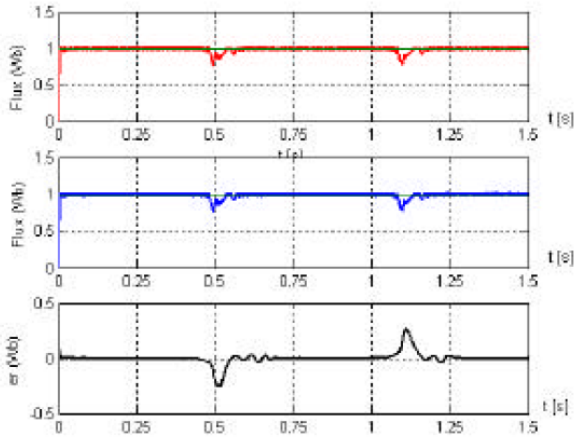


Fig. 6: The real estimated stator flux magnitude and estimation error

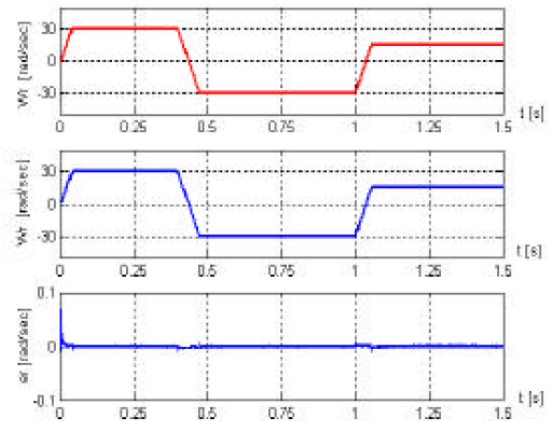


Fig. 9: Actual, estimated speed and estimation error

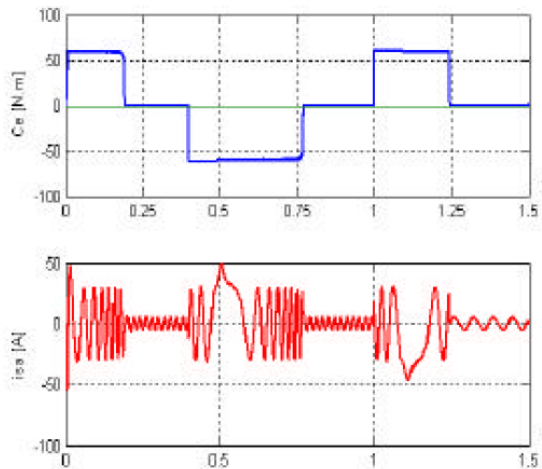


Fig. 7: Responses of electromagnetic torque and stator current

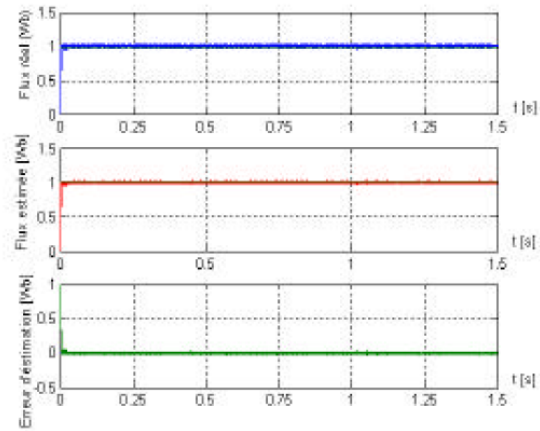


Fig. 10: Evolution of the stator flux magnitude

presented thereafter. The static and dynamic performances of the observer are analyzed according to the simulation of the following transients:

**Inversion of the speed:** To test the robustness of the system, we applied a changing of the speed reference from 157 rad/sec to -157 rad/sec at  $t=0.2s$ . Figure 5 presents the actual, estimated speeds  $\omega_r$ ,  $\hat{\omega}_r$ , respectively and the estimation error. Figure 6 presents actual flux  $\Psi_s$ . The estimated flux  $|\hat{\Psi}_s|$  and estimation error. The estimation algorithm is robust because the variation of the speed is important and the estimated speed follows the real speed when the motor starts and at the moment of speed inversion.

Figure 7 illustrates the response of stator current and the electromagnetic torque. It should be noted that the amplitude of the torque ripple is slightly higher.

Figure 8 illustrates the trajectory of the estimated stator flux; the deviation detected is caused by the instantaneous reversal of the speed of the load torque at the zero crossing of the speed.

**OPERATION AT LOW SPEED**

To test the speed estimation by using an adaptive observer, the simulation was established in low speed. Figure 9 and 10. Illustrate the simulation results of the process of speed estimation with a speed reference equal to  $\pm 30 \text{ rad sec}^{-1}$ .

**Variation of the load torque:** Figure 11 and Fig. 12 illustrate the simulation results after the introduction of load torque 25N.m (rated torque) between 0.5s and 1s after a leadless starting. We can see the insensibility of the control algorithm to load torque variation.

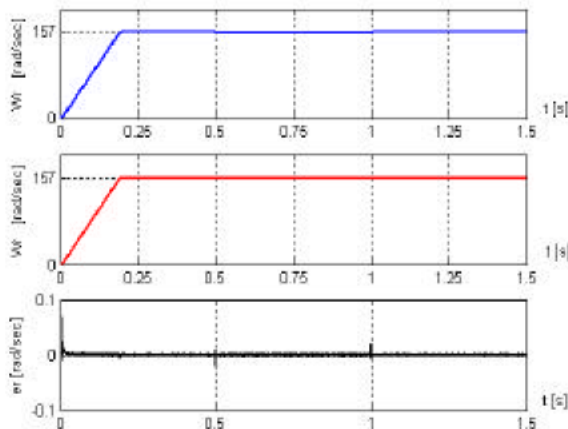


Fig. 11. Variation test of the load torque

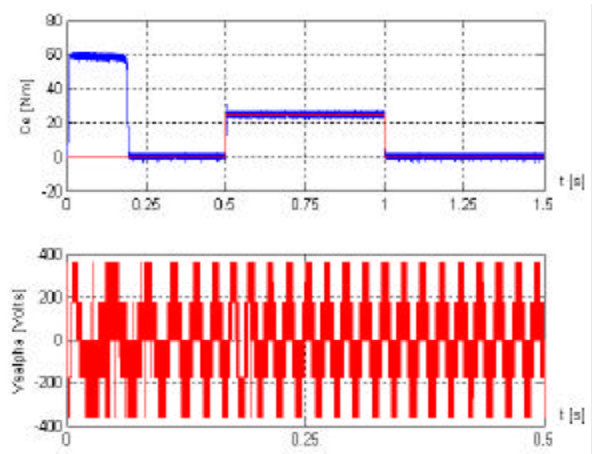


Fig. 12: Response of the electromagnetic torque and stator voltage

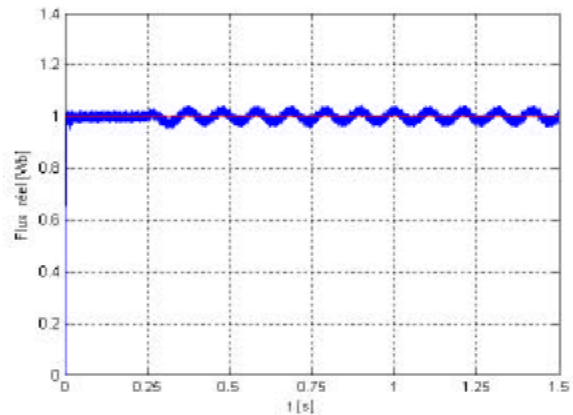


Fig. 13: Evolution of a real stator flux magnitude developed by the induction motor

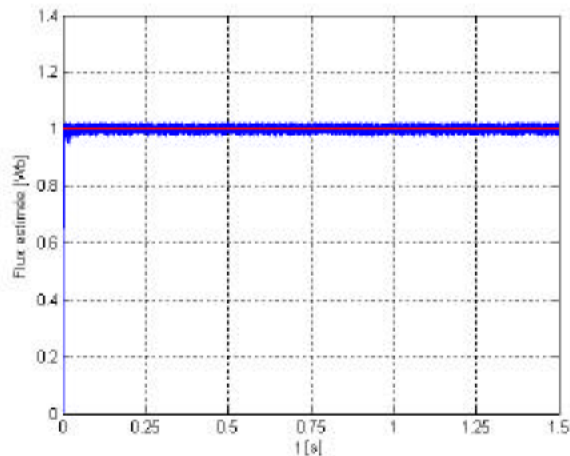


Fig. 14: Evolution of an estimated stator flux magnitude developed by the adaptive observer

**Effect of the stator resistance variation:** To highlight the effect of stator resistance, we carried out to vary the stator resistance.

Figure 13 and 14 illustrates the evolution of the estimated and the real magnitude of the stator flux with an increase of +100 % of the stator resistance at 0.25s. We note that according to these results that the observer corrects well the stator flux magnitude and follows its reference in established mode.

### CONCLUSION

We have presented in this study, the estimation of stator flux components and rotor speed using the adaptive observer. The estimation of these states allows a Direct Torque Control (DTC) sensorless drive with high performance to be realized. The adaptive observer uses an adaptation mechanism for the speed estimation when the load torque change, this approach relies on the improvement of an estimation of the components of the stator flux. An anti-windup PI regulator has been used to replace the classical PI controller in the speed control of a direct torque control. In conclusion, it seems that the anti-windup PI controller outperforms the classical PI controller in speed control of high performance DTC motor drive. This association makes the induction motor based DTC more robust and more stable.

### REFERENCES

Akin, B., 2003. State estimation techniques for speed sensorless field oriented control of induction motors, M.Sc. Thesis EE Department, METU.  
Bottiglieri, G., G. Scelba and G. Scarcella, 2003. Sensorless speed estimation in induction motor drives, IEEE. Electric Machines, IEMDC., pp: 624-630.

Canudas de wit, C., 2000. Modélisation contrôle vectoriel et DTC, Edition HARMES Science Europe, Ltd.  
Cao, Y., Z. Lin and D. G. Ward, 2002. An anti-windup approach to enlarging domain of attraction for linear systems subject to actuator saturation, IEEE. Trans. Automat Control, 47: 140-145.  
Casadei, D., F. Profum, G. Serra and A. Tani, 2002. FOC and DTC: Two viable schemes for induction motors torque control, IEEE. Trans. Ind. Applied, 17: 779-786.  
Casadei, D., G. Serra and A. Tani, 2003. Performance analysis of a speed-sensorless induction motor drive based on a constant-switching-frequency DTC scheme, IEEE. Trans. Ind. Applied, 39: 456-462.  
Elbuluk M.E. and M.D. Kankam, 1997. Speed sensorless induction motor drives for electrical actuators: Chemes, trends and tradeoffs, Prepared for the national aerospace and Electronics cosponsored by IEEE., Dayton, Ohio, pp:14-18.  
Lascu, C., I. Boldea and F. Blaabjerg, 2000. A modified direct torque control for induction motor sensorless drive, IEEE. Trans. Ind. Applied, 36: 122-130.  
Maes, J. and J. Melkebeek, 2000. Speed sensorless direct torque control of induction motors using an adaptive flux observer, Proc. IEEE. Trans. Ind. Applied, 36: 778-785.  
Takahashi, I. and T. Noguchi, 1986. A new quick-response and high efficiency control strategy of an induction machine, IEEE. Trans. Ind. Applied, 22: 820-827.  
Morand, F., 2005. Techniques d'observation sans capteur de vitesse en vue de la commande des machines asynchrones, Thèse de doctorat de L'institut National des Sciences Appliquées de Lyon, Janvier.  
Zaccarian L. and A. Teel, 2004. Nonlinear scheduled anti-windup design for linear systems, IEEE. Trans. Automat Control, 49: 2055-2061.